Available online at www.sciencedirect.com
SCIENCE DIRECT
Journal of Catalysis 238 (2006) 214–220
JOURNAL OF CATALYSIS
www.elsevier.com/locate/jcat

Photoactive sites on pure silica materials for nonoxidative direct methane coupling

Leny Yuliati [a], Masanori Tsubota [a], Atsushi Satsuma [a], Hideaki Itoh [b], Hisao Yoshida [b,*]

[a] *Department of Applied Chemistry, Graduate School of Engineering, Nagoya University, Furo-cho, Chikusa-ku, Nagoya 464-8603, Japan*
[b] *Division of Environmental Research, EcoTopia Science Institute, Nagoya University, Furo-cho, Chikusa-ku, Nagoya 464-8603, Japan*

Received 15 September 2005; revised 30 November 2005; accepted 5 December 2005

Available online 10 January 2006

Abstract

Some pure silica materials, such as amorphous silica and mesoporous silica (MCM-41, FSM-16), were examined as photocatalysts for nonoxidative direct methane coupling around room temperature. It was confirmed that these materials exhibited photoactivity for the reaction around room temperature to produce mainly ethane and hydrogen, and that mesoporous silica, FSM-16, exhibited the highest activity among them. The photoactive sites on these pure silica materials were formed through dehydroxylation of the surface hydroxyl groups at high temperature (e.g., 1073 K) before the photoreaction. The linear relationship was obtained between the area intensity of the nonbridging oxygen hole center (NBOHC) band in diffuse–reflectance UV–visible spectra and the photoactivities in the nonoxidative direct methane coupling, showing that the NBOHCs, which would be generated together with the E′ center, were the photoactive sites for this reaction.

Keywords: Nonoxidative direct methane coupling; Photocatalyst; Mesoporous silica materials; Surface defect; NBOHC

1. Introduction

Because methane is still abundant as natural gas and methane hydrate, methane is widely used in the production of energy and chemicals, and various methods of improving the efficiency of its use have been examined. Among these, the production of higher hydrocarbons from the methane remains a leading challenge [1–4]. Steam reforming of methane, currently the major route for methane conversion, can be represented as follows: $CH_4 + H_2O \rightarrow CO + 3H_2$. This process produces synthesis gas that can be further processed into methanol, ammonia, higher hydrocarbons, and so on. But this is an indirect route through an oxidation process followed by a reduction process, and the direct conversion of methane is desired to obtain higher hydrocarbons. Although the oxidative coupling of methane (OCM) in the presence of oxygen has attracted much interest as a method of direct methane conversion, it tends to produce CO_x molecules as well as the expected hydrocarbons. Another route is direct methane coupling under nonoxidative conditions,

$$2CH_4 \rightarrow C_2H_6 + H_2, \quad \Delta G_{(298\,K)} = 68.6\ \text{kJ/mol}.$$

Unfortunately, this reaction occurs only at high temperature, because high energy is necessary to overcome the thermodynamic barriers.

We have reported that the use of photoenergy through a photocatalyst is a plausible method for letting the reaction occur at room temperature [5–13]. To date, several varieties of silica-based photocatalysts have been developed, including silica–alumina [5–7], silica-supported zirconia [8,9], silica-supported magnesia [10], silica–alumina–titania [11,12], and also zeolites [13], which exhibit activity under UV irradiation at room temperature.

It is well known that silica is basically inert for many reactions. However, silica exhibits measurable activities for some catalytic [14–23] and photocatalytic [5–12,24–31] reactions, albeit at a lower level than most of other catalysts and photocatalysts. Recently, pure silica has become of interest in promoting photocatalytic reactions under UV irradiation, including photometathesis of propene [24–27], photoepoxidation of

* Corresponding author. Fax: +81 52 789 5849.
E-mail address: h-yoshida@esi.nagoya-u.ac.jp (H. Yoshida).

0021-9517/$ – see front matter
doi:10.1016/j.jcat.2005.12.002

propene [28–30], and photooxidation of CO [31], as well as in the nonoxidative direct coupling of methane [5–12].

In the present study, we investigated the photoactivity of pure silica materials, such as amorphous silica and mesoporous silica materials (MCM-41 [32,33] and FSM-16 [34,35]), for nonoxidative direct methane coupling and discussed the active sites on the pure silica materials.

2. Experimental

2.1. Materials

The amorphous silica sample was prepared by the sol–gel method [28]. The mesoporous silica samples (MCM-41 and FSM-16) were prepared as described previously [24], using hexadecyltrimethylammonium bromide [$C_{16}H_{33}(CH_3)_3N^+Br^-$] (Kishida) as a template and highly pure silicate soda (SiO_2/Na_2O ca. 2.59, Al 0.6 ppm, Fe 0.4 ppm, donated from Fuji Silysia) as a silica source.

2.2. Characterization of catalysts

BET specific surface area of the amorphous silica sample was calculated from the amount of desorbed nitrogen that adsorbed in a flow of He–N_2 (70–30%) at 77 K. Before the measurement, the sample was heated at 673 K for 30 min in a flow of He. On the other hand, the adsorption/desorption isotherms of nitrogen for the mesoporous silica samples were recorded on an automatic gas adsorption apparatus BELSORP 28SA after evacuation threatment of the sample at 673 K for 1 h. The pore size distribution of the mesoporous silica samples was calculated by the Dollimore–Heal (DH) method from the adsorption isotherm.

Powder X-ray diffraction (XRD) patterns were recorded at room temperature on a RINT 1200 diffractometer using Ni-filtered Cu-K_α radiation (40 kV, 20 mA). Diffuse–reflectance UV–visible spectra were recorded at room temperature on a JASCO V-550 equipped with an integrating sphere covered with $BaSO_4$ using a specially designed in situ cell. $BaSO_4$ was used as a reference sample. Before the UV–visible spectrum was recorded, the sample was heated in air up to 1073 K, then evacuated. Subsequently, the sample was treated in 13.3 kPa of oxygen atmosphere at 1073 K for 1 h to clean up the surface, followed by evacuation at 1073 K for 1 h to remove the molecules and complete the surface dehydration. Then the sample was transferred to the optical part of the cell without being exposed to the atmosphere.

2.3. Photocatalytic reaction

The reaction tests were carried out in a closed quartz reaction vessel in the similar way to the previous studies [5–13]. The catalyst sample (0.2 g) was spreaded over the flat bottom (14 cm^2) of the reactor (30 cm^3) and pretreated under 13.3 kPa of oxygen atmosphere for 1 h at 773 or 1073 K, followed by evacuation for 1 h at 773 or 1073 K. After the sample was cooled to room temperature, 200 μmol of methane was introduced to the reactor. The photoreaction was carried out on photoirradiation from beneath by a 300 W Xe lamp for 3 h (at 17.5 A, 15 V, intensity of light measured at the reactor in the range of 220–300 nm of 10 mW/cm^2). The products in the gas phase were analyzed by gas chromatography, then evacuated. The adsorbed products on the catalyst were thermally desorbed by heating at 573 K for 15 min and collected for analysis by gas chromatography. After another evacuation, the sample was heated at 773 K for 1 h in the presence of oxygen in order to check the existence of strongly adsorbed products that would be detected as CO_2. Two types of detectors were used to analyze the products: a thermal conductivity detector with an Ar carrier to detect hydrogen and CO_2, and a flame ionization detector to detect hydrocarbons.

3. Results

3.1. Characterization

The synthesized mesoporous silica samples MCM-41 and FSM-16 demonstrated type IV isotherms of the IUPAC classification. In terms of pore size distribution, both samples exhibited uniform pore diameter, 2.7 nm for MCM-41 and 2.5 nm for FSM-16. Table 1 gives the BET surface area of the silica samples along with the pore diameter. As reported previously [24,25,32–35], MCM-41 and FSM-16 exhibited high surface areas.

In the XRD patterns, MCM-41 and FSM-16 exhibited three well-resolved diffraction lines in the low range 2θ region (1.5°–6°) indexed as (100), (110), and (200) diffraction lines of two-dimensional hexagonal unit cells, suggesting that these samples have a highly ordered hexagonal structure, in good agreement with previous studies [24,32–35]. From the characterization results mentioned above, it is clear that the MCM-41 and FSM-16 samples have been successfully synthesized as mesoporous silica materials.

3.2. UV absorption spectra

Fig. 1 shows the diffuse–reflectance UV–visible spectra of the amorphous silica, MCM-41, and FSM-16 samples. All of the samples showed a broad and weak absorption band at around 200–300 nm that has been assigned to the surface defects on silica materials [25,36–45]. The intensities of the spectra varied, implying that the number of surface defects would be different among the samples. The area intensity of the entire band was in the following order: FSM-16 > MCM-41 > amorphous silica.

The broad absorption band seems to consist of some bands that can be simulated by using some Gaussian curves. The

Table 1
BET specific surface area and pore diameter of the silica samples

Sample	BET specific surface area (m^2/g)	Pore diameter (nm)
Amorphous silica	554	–[a]
MCM-41	915	2.7
FSM-16	994	2.5

[a] Not recorded.

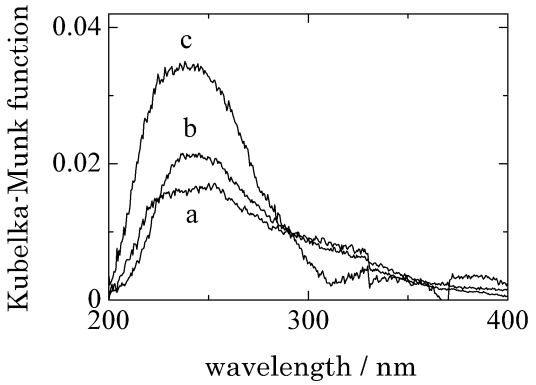

Fig. 1. Diffuse–reflectance UV–visible spectra of the pure silica samples: (a) amorphous silica, (b) MCM-41, and (c) FSM-16. The samples were pretreated at 1073 K before recording the spectra.

Table 2
The best parameters for the curve fitting of diffuse reflectance UV–visible spectra by using Gaussian functions[a]

Parameter	Sample	Gaussian			
		G_1	G_2	G_3	G_4
Center position (eV)		4.1[b]	4.8	5.05	5.55[c]
FWHM (eV)		1.3	1.05	1.0	0.8
Maximum height (10^{-2})	Amorphous silica	0.79	0.14	0.89	0.88
	MCM-41	0.54	0.88	0.64	0.99
	FSM-16	0.22	1.21	1.64	1.88
Area (arb.u.)	Amorphous silica	1.63	0.18	0.94	0.60
	MCM-41	1.17	1.08	0.67	0.72
	FSM-16	0.47	1.49	1.73	1.27

[a] The samples were pretreated at 1073 K before recording the diffuse–reflectance UV–visible spectra.
[b] The energy position for G_1 employed was 4.2 for the spectrum of the amorphous silica sample.
[c] The energy position for G_4 employed was 5.4 for the spectrum of the MCM-41 sample.

Gaussian function for curve-fitting of diffuse–reflectance UV–visible spectra can be expressed as follows:

$$G_n(x) = he^{-\frac{4\ln 2(x-E_n)^2}{w^2}},$$

where x represents energy of the light (eV), h is maximum height, E_n is the center position of each band (eV), and w is full width at half maximum (FWHM) (eV).

Fig. 2 shows the best simulation of the diffuse–reflectance UV–visible spectra of the samples. Table 2 describes the best-fitting parameter sets. Note that the exact measurement in the short-wavelength region, such as 200–220 nm (6.2–5.6 eV) is difficult due to the weak intensity of the incident light. As shown in Fig. 2, the broad absorption band was deconvoluted into at least four bands using the reported parameters of the center position and FWHM for the defects on silica [25,36–45]. The bands were centered at 4.1 eV (302 nm, G_1), 4.8 eV (258 nm, G_2), 5.05 eV (245 nm, G_3), and 5.55 eV (223 nm, G_4). The first band (G_1) can be attributed to intrinsic centers [36]. The second band (G_2) has been studied by many techniques and assigned to the NBOHC [25,37–41]. The third band (G_3) corresponds to a kind of surface center called dioxasilirane group [37,42]. The other suggested model for the site absorbing UV light around 5 eV is an oxygen divacancy [38,43]. The fourth band (G_4) possibly could be assigned to the surface silanone group (i.e. the Si=O double bond [37,44]), or possibly to the surface peroxy radical and the E′ center with a neighboring OH group, which have been suggested to show an absorption band around 5.4 eV [37,38,45]. These diffuse–reflectance UV–visible spectra confirm the presence of four (or more) kinds of optically active defects absorbing UV light. However, it is known that the photoabsorbing sites do not always function as photocatalytic active sites.

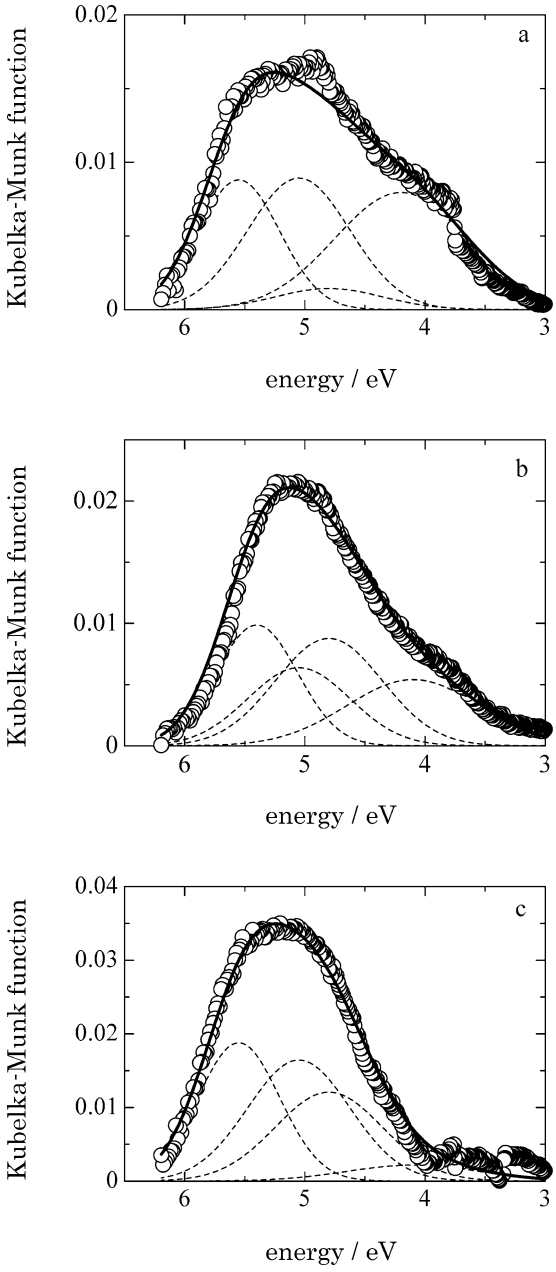

Fig. 2. The best results in the curve fitting analysis for the diffuse–reflectance UV–visible spectra of (a) amorphous silica (b) MCM-41, and (c) FSM-16. The symbols show the experimental spectra and the solid lines show the simulated spectra, which are composed of four Gaussian functions (broken lines, see text and Table 2).

Table 3
Photoactivities of the samples in the nonoxidative direct methane coupling[a]

Entry	Sample	Pretreatment temperature (K)	Yield of gaseous phase products (10^{-2} C%[b])			Yield of thermally desorbed products[c] (10^{-2} C%[b])		Total yield (10^{-2} C%[b])	Yield of H_2 (10^{-2} μmol)	
			C_2H_4	C_2H_6	C_3H_8	C_2H_4	C_2H_6		Experimental	Theoretical[d]
1	Amorphous silica	773	0.03	0.10	n.d.	n.d.	n.d.	0.13	n.d.	0.16
2	MCM-41	773	n.d.	0.92	0.11	n.d.	n.d.	1.03	n.d.	1.08
3	FSM-16	773	n.d.	1.63	0.03	n.d.	n.d	1.67	n.d.	1.67
4	Amorphous silica	1073	n.d.	0.42	0.05	n.d.	n.d.	0.45	n.d.	0.46
5	MCM-41	1073	n.d.	4.23	0.17	n.d.	n.d.	4.40	tr.	4.44
6	FSM-16	1073	n.d.	5.40	0.28	n.d.	n.d.	5.67	tr.	5.78
7	FSM-16[e]	1073	n.d.	9.46	0.92	0.04	tr.	10.41	10.1	10.76

[a] Reaction temperature, ca. 310 K; sample, 0.2 g; methane, 200 μmol; irradiation time, 3 h. H_2 was analyzed by TCD (detection limit, 0.04 μmol), hydrocarbons were analyzed by FID (experimental error, <4%). tr. = trace, n.d. = not detectable.
[b] Based on the initial amount of methane.
[c] The products were obtained by the desorption procedure at 573 K for 15 min.
[d] Calculated from the total yield of gaseous products and thermally desorbed products.
[e] Another sample of FSM-16 prepared separately, irradiation time was 24 h.

3.3. Nonoxidative direct methane coupling

Table 3 gives the results of photocatalytic nonoxidative direct methane coupling over the amorphous and mesoporous silica samples. Different pretreatment temperatures (773 and 1073 K) were used to study the effect of pretreatment temperature on the activity of the samples. Entries 1–3 and entries 4–6 show the activities of silica samples pretreated at 773 and 1073 K, respectively. It can be confirmed that no product was detected in the dark. All of the silica samples exhibited the activities for photoreaction, and the dominant product was ethane as a gaseous product. No product was collected from all of the samples by a thermal desorption procedure at 573 K for 15 min, except after photoirradiation for 24 h, in which a trace amount of thermally desorbed product, such as ethene, was obtained (Table 3, entry 7). Moreover, only a trace amount of CO_2 was obtained after successive heating in the presence of oxygen at 773 K for 1 h, indicating that strongly adsorbed products remained but only at negligible amounts. These findings suggest that the products were hardly adsorbed on the silica materials during photoreaction, and thus catalyst deactivation during the photoreaction would be expected to be low.

Only a trace amount of hydrogen was observed on the mesoporous silica samples (Table 3, entries 5 and 6) after photoreaction for 3 h, because of the low sensitivity of gas chromatography for hydrogen. However, hydrogen was detected almost stoichiometrically after irradiation for 24 h on the FSM-16 sample (Table 3, entry 7). Thus, the main reaction can be described as follows:

$$2CH_4 \rightarrow C_2H_6 + H_2.$$

The findings mentioned earlier suggest that the reaction proceeded photocatalytically.

The silica samples pretreated at 1073 K showed higher activities than those pretreated at 773 K. Varying the pretreatment temperature did not change the order of the activities among the silica samples; for both pretreatment temperatures, the activities of the silica samples were in the following order: FSM-16 > MCM-41 > amorphous silica. This suggests that the photoactive sites on these samples were generated similarly by pretreatment at high temperature, implying that these samples have the same kinds of photoactive sites. Also note that the mesoporous silica samples seemed to show higher activity than those of other silica-based photocatalysts, that is, the highly dispersed metal oxide on silica systems [5–10]. This finding is discussed in more detail in Section 4.

4. Discussion

The active centers on silica for some photocatalytic reactions have been investigated by various methods. In the case of photooxidation reaction, for example, it was suggested that the hole center of O^- photoformed from lattice oxygen of silica would react with O_2 to form O_3^- species, which would further react with the substrate [31]. In a nonoxidative photoreaction without oxidant molecules, such as in photometathesis of propene, the active sites on silica was proposed to be a type of surface defect, that is, NBOHC accompanied by an E′ center. The NBOHC that can be photoexcited under UV irradiation showed an absorption band at around 250 nm, in agreement with the effective wavelength region for the photometathesis, suggesting the role of NBOHC as the initial photoactive site for photoreaction; these findings have been supported by IR, ESR, and photoluminescence spectroscopy [25,26]. In the present study, the condition of the reaction was similar to that of the propene photometathesis, in which no oxidant molecules were introduced into the reaction system.

As shown in Table 3, pretreatment at higher temperature contributed to the higher activity in the photoreaction. This suggests that the generation of photoactive sites on the silica samples was closely related to the dehydroxylation of surface hydroxyl groups on them. It has been reported that the surface hydroxyl groups on silica materials are further dehydroxylated at the higher evacuation temperatures to produce the surface active sites exhibiting IR bands at 891 and 910 cm^{-1} [25,39,46–48]. These surface active sites have been revealed as two radical sites, ≡Si–O· (NBOHC) and ·Si≡ (E′ center), as shown in Scheme 1 [25,46], the first of which contributes

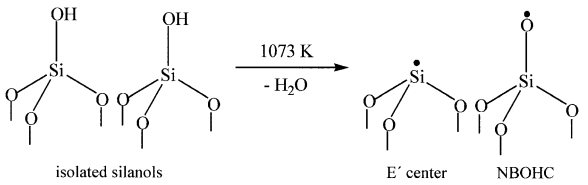

Scheme 1. The formation of the surface active sites on silica materials during the evacuation treatment a high temperature.

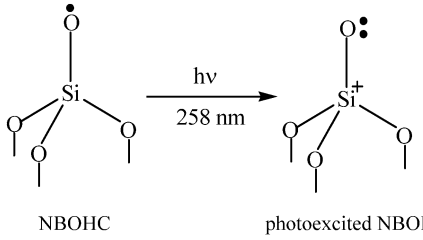

Scheme 2. The photoexcitation of NBOHC.

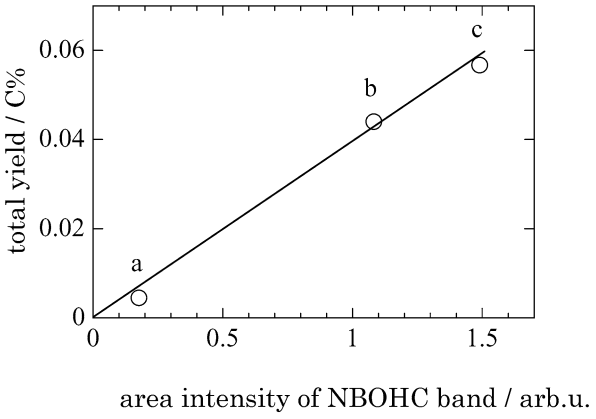

Fig. 3. The relationship between the area intensity of the NBOHC band in the diffuse–reflectance UV–visible spectra of the silica samples and the total yield in the nonoxidative direct methane coupling on them. The each plot corresponds to (a) amorphous silica, (b) MCM-41, and (c) FSM-16. The data were taken from Tables 2 and 3.

to the IR bands [25]. Thus, the photoactive sites for nonoxidative direct methane coupling, which are generated through evacuation at high temperature, are proposed to be the surface active sites, such as NBOHC generated together with the E′ center.

As suggested in a previous study [25], under UV light below ca. 390 nm, the initial photoexcitation step occurs in the NBOHC, corresponding to a charge transfer from bonding orbital of Si–O to 2p nonbonding orbital of nonbridging oxygen as shown in Scheme 2 [25,47]. Because nonoxidative direct methane coupling could not start without photoirradiation, the excitation of the NBOHC is proposed to be the initial step in the reaction. To evaluate the possibility that the NBOHC are the photoactive sites for nonoxidative direct methane coupling, we analyzed diffuse–reflectance UV–visible spectra of the silica materials. As shown in Table 2 and Fig. 2, these spectra demonstrated the presence of surface defects absorbing UV light, such as the NBOHC. It is clear that the amount of the generated NBOHC was in the following order: FSM-16 > MCM-41 > amorphous silica, which is in good agreement with previous studies using ESR and IR [25]. Thus, the area intensity of the NBOHC band and the photoactivity of the silica samples for the reaction were plotted, as shown in Fig. 3. It was found that the activity of the silica materials increased proportionally with increasing area intensity of the NBOHC band in the diffuse–reflectance UV–visible spectra. This good linear relationship strongly suggests that the NBOHC are the photoactive sites in silica materials for nonoxidative direct methane coupling. In addition, no good relationship was found between the activity of the silica samples and the amount of other species detected by diffuse–reflectance UV–visible spectroscopy. The present study has clarified that the NBOHC should act as photoactive sites not only for metathesis, but also for nonoxidative direct methane coupling.

A mechanism for the initial activation in the present nonoxidative direct methane coupling can be proposed as shown in Scheme 3. As mentioned earlier, the first step would be the photoexcitation of NBOHC. The methane would interact with the photoexcited NBOHC, followed by the formation of methyl and hydrogen radicals, which would further react with methane to form higher hydrocarbons, such as ethane, and hydrogen.

The energy for the excitation of the NBOHC corresponds to 258-nm wavelength light. This energy is close to those of previously reported silica–alumina [5], silica-supported zirconia [8], and silica-supported magnesia [10], which exhibited photoabsorption bands or photoluminescence excitation bands at around 230, 240, and 250 nm, respectively. These highly dispersed metal oxides on silica supports had higher activity than the bare amorphous silica support. On the other hand, the present study found that the mesoporous silica materials MCM-41 and FSM-16 had higher activity than silica-based photocatalysts.

To evaluate whether the NBOHC with E′ center in pure silica materials or the surface Si–O–M bond in the silica-based photocatalysts (highly dispersed metal oxide species on silica) is the more effective photoactive site, we compared the

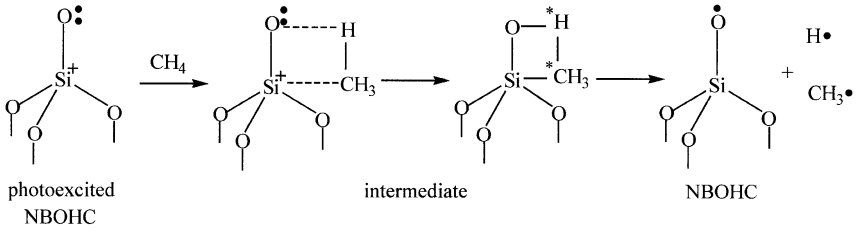

Scheme 3. The proposed mechanism for the initial activation in the nonoxidative direct methane coupling over pure silica materials.

specific activity of these photoactive sites by estimating their turnover frequency (TOF). For the comparison, the reaction tests were carried out carefully on FSM-16 and MgO/SiO_2 (Mg content, 0.5 mol%) samples under the same conditions, using the irradiation from a Xe lamp with almost the same intensity (around 10 mW/cm^2 for the range of 220–300 nm) for 24 h. The TOF was defined as the amount of H_2 produced per hour per amount of active sites. In previous studies, the amount of NBOHC in FSM-16 pretreated at 1073 K was estimated as around 35 μmol/g [25]. On the other hand, the amount of the Si–O–Mg linkages on MgO/SiO_2 (0.5) was defined as the amount of Mg under assumption that all of the added Mg formed highly dispersed Si–O–Mg linkages [10]. The TOF over the FSM-16 sample was determined to be about 6×10^{-4} h^{-1}, whereas the TOF over the MgO/SiO_2 (0.5) sample was 2×10^{-4} h^{-1}. Although these values were close to one another in the same order, the NBOHC with E′ center in FSM-16 showed a higher specific activity than the Si–O–M bond under the present assumption. As mentioned earlier, only a small amount of NBOHC was formed on amorphous silica. Thus, the addition of metal oxide to form the highly dispersed Si–O–M linkages is important to increase the photoactivity of amorphous silica, as proposed previously [10]. In the case of mesoporous silica, high photoactivity can be obtained even without adding any metal oxides. This suggests that the characteristic mesopore structure consisting of thin silica walls plays an important role in forming the photoactive sites (i.e., NBOHC with E′ center).

5. Conclusions

Based on the findings of our study, we can state the following conclusions:

(i) On photoirradiation, pure silica materials evacuated at high temperature (e.g., 1073 K) promoted nonoxidative direct methane coupling.
(ii) The activity was in the following order: FSM-16 > MCM-41 > amorphous silica. The mesoporous silica materials exhibited higher activity than the reported silica-based photocatalysts.
(iii) The same kinds of photoabsorption sites were generated through the dehydroxylation of the surface hydroxyl groups at high temperature on these silica materials. One of these, a kind of surface defect on silica, NBOHC accompanied by E′ center, was identified as the photoactive sites for nonoxidative direct methane coupling.

Acknowledgments

This work was partially supported by a Grant-in-Aid for Scientific Research on Priority Areas (417) from the Japanese Ministry of Education, Culture, Sports, Science and Technology. The authors thank Fuji Silysia Chemical Ltd for their kind donation of high-purity silicate soda.

References

[1] H.D. Gesser, N.R. Hunter, Catal. Today 42 (1998) 183.
[2] J.H. Lunsford, Catal. Today 63 (2000) 165.
[3] Y. Xu, X. Bao, L. Lin, J. Catal. 216 (2003) 386.
[4] T.V. Choudhary, E. Aksoylu, D.W. Goodman, Catal. Rev. 45 (2003) 151.
[5] H. Yoshida, N. Matsushita, Y. Kato, T. Hattori, Phys. Chem. Chem. Phys. 4 (2002) 2459.
[6] Y. Kato, H. Yoshida, T. Hattori, Chem. Commun. (1998) 2389.
[7] H. Yoshida, Y. Kato, T. Hattori, Stud. Surf. Sci. Catal. 130 (2000) 659.
[8] H. Yoshida, M.G. Chaskar, Y. Kato, T. Hattori, J. Photochem. Photobiol. A 160 (2003) 47.
[9] H. Yoshida, M.G. Chaskar, Y. Kato, T. Hattori, Chem. Commun. (2002) 2014.
[10] L. Yuliati, T. Hattori, H. Yoshida, Phys. Chem. Chem. Phys. 7 (2005) 195.
[11] Y. Kato, N. Matsushita, H. Yoshida, T. Hattori, Catal. Commun. 3 (2002) 99.
[12] H. Yoshida, N. Matsushita, Y. Kato, T. Hattori, J. Phys. Chem. B 107 (2003) 8355.
[13] Y. Kato, H. Yoshida, A. Satsuma, T. Hattori, Microporous Mesoporous Mater. 51 (2002) 223.
[14] E.W. Bittner, B.C. Bockrath, J.M. Solar, J. Catal. 149 (1994) 206.
[15] K. Vikulov, G. Martra, S. Collucia, D. Miceli, F. Arena, A. Parmaliana, E. Paukshtis, Catal. Lett. 37 (1996) 235.
[16] Y. Sakata, M.A. Uddin, A. Muto, K. Koizumi, Y. Kanda, K. Murata, J. Anal. Appl. Pyrolysis 43 (1997) 15.
[17] F. Arena, N. Giordano, A. Parmaliana, J. Catal. 167 (1997) 66.
[18] G. Fornasari, F. Trifirò, Catal. Today 41 (1998) 443.
[19] T. Yamamoto, T. Tanaka, T. Funabiki, S. Yoshida, J. Phys. Chem. B 102 (1998) 5830.
[20] Y. Tanaka, N. Sawamura, M. Iwamoto, Tetrahedron Lett. 39 (1998) 9457.
[21] T. Yamamoto, T. Tanaka, S. Inagaki, T. Funabiki, S. Yoshida, J. Phys. Chem. B 103 (1999) 6450.
[22] R. Bal, B.B. Tope, T.K. Das, S.G. Hegde, S. Sivasanker, J. Catal. 204 (2001) 358.
[23] J. Haber, K. Pamin, L. Matachowski, D. Mucha, Appl. Catal. A 256 (2003) 141.
[24] Y. Inaki, H. Yoshida, K. Kimura, S. Inagaki, Y. Fukushima, T. Hattori, Phys. Chem. Chem. Phys. 2 (2000) 5293.
[25] Y. Inaki, H. Yoshida, T. Yoshida, T. Hattori, J. Phys. Chem. B 106 (2002) 9098.
[26] Y. Inaki, H. Yoshida, T. Hattori, J. Phys. Chem. B 104 (2000) 10304.
[27] H. Yoshida, K. Kimura, Y. Inaki, T. Hattori, Chem. Commun. (1997) 129.
[28] H. Yoshida, C. Murata, T. Hattori, J. Catal. 194 (2000) 364.
[29] H. Yoshida, T. Shimizu, C. Murata, T. Hattori, J. Catal. 220 (2003) 226.
[30] C. Murata, H. Yoshida, J. Kumagai, T. Hattori, J. Phys. Chem. B 107 (2003) 4364.
[31] A. Ogata, A. Kazusaka, M. Enyo, J. Phys. Chem. 90 (1986) 5201.
[32] J.S. Beck, J.C. Vartuli, W.J. Roth, M.E. Leonowicz, C.T. Kresge, K.D. Schmitt, C.T.-W. Chu, D.H. Olson, E.W. Shephard, S.B. McCullen, J.B. Higgins, J.L. Schlenker, J. Am. Chem. Soc. 114 (1992) 10834.
[33] C.T. Kresge, M.E. Leonowicz, W.J. Roth, J.C. Vartuli, J.S. Beck, Nature 359 (1992) 710.
[34] S. Inagaki, Y. Fukushima, K. Kuroda, J. Chem. Soc., Chem. Commun. (1993) 680.
[35] S. Inagaki, A. Koiwai, N. Suzuki, Y. Fukushima, K. Kuroda, Bull. Chem. Soc. Jpn. 69 (1996) 1449.
[36] S. Agnello, B. Boizot, J. Non-Cryst. Solids 322 (2003) 84.
[37] L. Skuja, J. Non-Cryst. Solids 239 (1998) 16.
[38] L. Skuja, in: G. Pacchioni, L. Skuja, D.L. Griscom (Eds.), Defects in SiO_2 and Related Dielectrics: Science and Technology, Kluwer Academic, Dordrecht, 2000, p. 73.
[39] L. Skuja, R. Silin, Phys. Status Solidi A 56 (1979) 1.
[40] D.L. Griscom, J. Ceram. Soc. Jpn. 99 (1991) 899.
[41] L. Skuja, K. Tanimura, N. Itoh, J. Appl. Phys. 80 (1996) 3518.
[42] A.A. Bobyshev, V.A. Radtsig, Khim. Phys. 7 (1998) 950.

[43] H. Nishikawa, R. Tohmon, Y. Ohki, K. Nagasawa, Y. Hama, J. Appl. Phys. 65 (1989) 4672.
[44] V.A. Radtsig, I.N. Senchenya, Russ. Chem. Bull. 45 (1996) 1849.
[45] A.A. Bobyshev, V.A. Radtsig, Fiz. Khim. Stekla 14 (1998) 501.
[46] Y.D. Glinka, S.-H. Lin, L.-P. Hwang, Y.-T. Chen, J. Phys. Chem. B 104 (2000) 8652.
[47] L. Skuja, Solid State Commun. 84 (1992) 613.
[48] I.-S. Chuang, G.E. Maciel, J. Phys. Chem. B 101 (1997) 3052.